Supplementary Information

Effects of single and double active sites of Cu oxide clusters over MFI zeolite for direct conversion of methane to methanol: DFT calculations

*Watinee Nunthakitgoson,[a] Anawat Thivasasith,[*a] Thana Maihom,[b] and Chularat Wattanakit[a]*

[a] Department of Chemical and Biomolecular Engineering, School of Energy Science

and Engineering, Vidyasirimedhi Institute of Science and Technology, Rayong,

21210, Thailand.

[b] Department of Chemistry, Faculty of Liberal Arts and Science, Kasetsart University,
Kamphaeng Saen Campus, Nakhon Pathom 73140, Thailand.
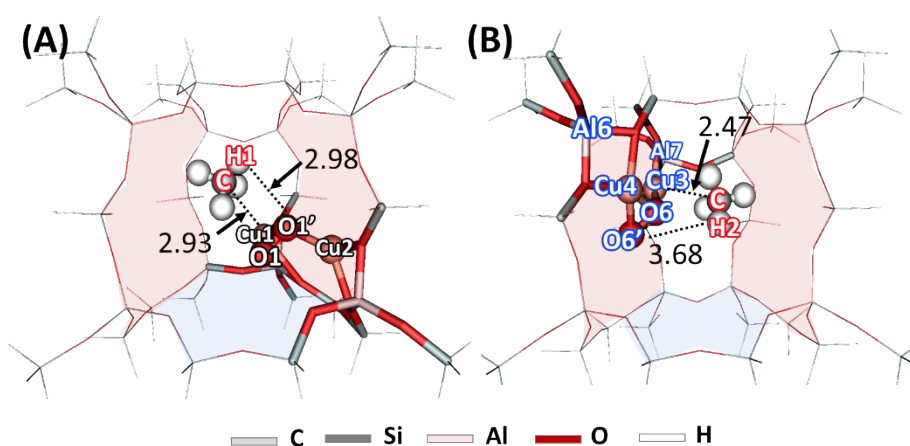
Corresponding Author's E-mail: anawat.t@vistec.ac.th

Fig. S1. Optimized structures of the adsorption state of methane on the single active site of A) [Cu(μ-1,2-peroxo)Cu]$^{2+}$@Al1'-Al12'/MFI, and B) [Cu(μ-1,2-peroxo)Cu]$^{2+}$@Al6-Al7/MFI calculated in the triplet spin ground state, and red and blue areas represent straight and zigzag channels, respectively (the unit of distance is in an angstrom).
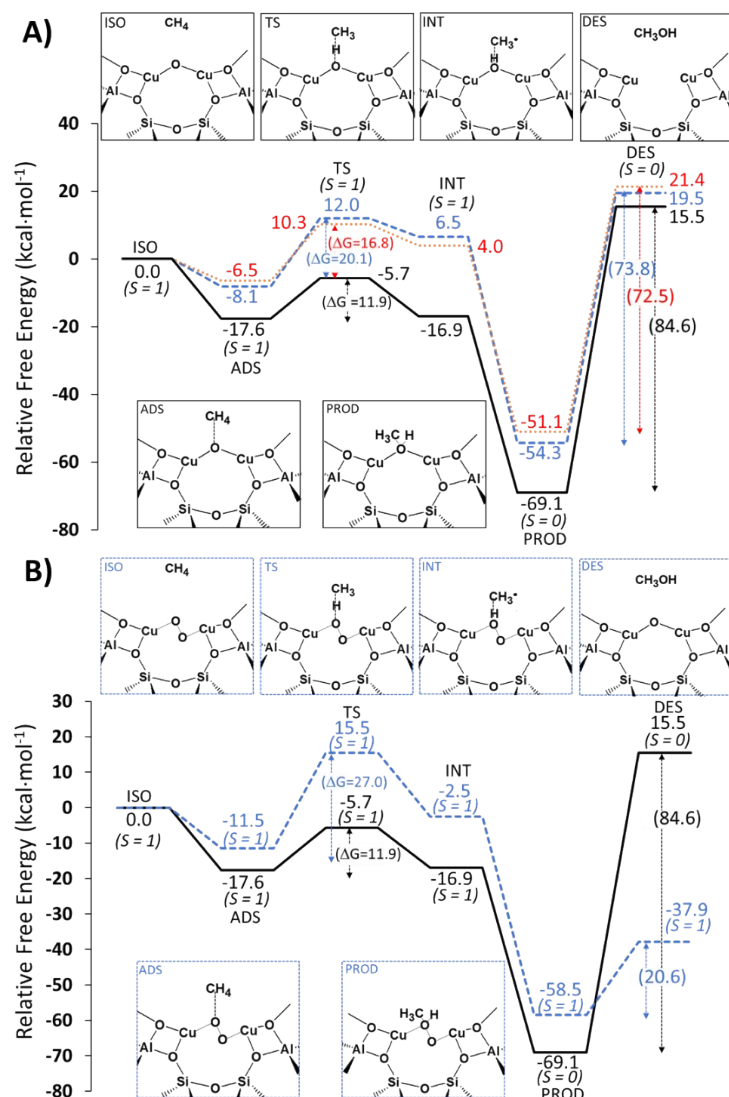
Fig. S2 Free energy profile ($\Delta G_{298.15}$) of overall steps of the direct conversion of methane to methanol on different Cu oxide clusters over MFI framework: A) comparison pathways of methane to methanol on single active site of $[Cu(\mu\text{-}O)Cu]^{2+}@Al1'\text{-}Al12'/MFI$ (blue dash line), $[Cu(\mu\text{-}O)Cu]^{2+}@Al6\text{-}Al7/MFI$ (red dot line), and on double active sites of $2[Cu(\mu\text{-}O)Cu]^{2+}/MFI$ (black line), B) comparison pathways of methane to methanol on $2[Cu(\mu\text{-}1,2\text{-peroxo})Cu]^{2+}/MFI$ (blue dash line) and $2[Cu(\mu\text{-}O)Cu]^{2+}/MFI$ (black line).

Structure details of single active site of [Cu(μ-O)Cu]$^{2+}$@Al1'-Al12'/MFI and [Cu(μ-O)Cu]$^{2+}$@Al6-Al7/MFI and double active sites 2[Cu(μ-O)Cu]$^{2+}$/MFI and 2[Cu(μ-1,2-peroxo)Cu]$^{2+}$/MFI

The confinement effect of zeolite cavities has important stabilization effect to the bond length and bond angle of the Cu active site in zeolite. For the single active site of Cu oxide cluster located at the intersection between straight and zigzag channel of the MFI frameworks, the pore size of zeolite quite large compare with the small size of single active site of Cu oxide cluster, thus, the confinement effect of zeolite is not too much effect to the structure of the single active site of Cu oxide cluster. Therefore, the Cu$\cdots$O$_{oxo}$ bond length of single active sites of [Cu(μ-O)Cu]$^{2+}$@Al1'-Al12'/MFI and [Cu(μ-O)Cu]$^{2+}$@Al6-Al7/MFI are approximately 1.89 Å. The bond angles of ∠Cu1O1Cu2 of [Cu(μ-O)Cu]$^{2+}$@Al1'-Al12'/MFI and ∠Cu3O6Cu4 of [Cu(μ-O)Cu]$^{2+}$@Al6-Al7/MFI are in the range of 150 and 156 °, respectively (Tables S1 and S2). While the double active site of Cu oxide cluster in zeolite framework, the confinement effect of zeolite is effect to the bond length and bond angle of double active site of Cu oxide cluster. For the double active sites of 2[Cu(μ-O)Cu]$^{2+}$/MFI, the average Cu$\cdots$O$_{oxo}$ bond length is shortened from 1.89 to 1.77 Å and the bond angle of ∠ CuO$_{oxo}$Cu is narrowing from the range of 150-156° to 142-143° compared with the single active site model (Table S3). For the 2[Cu(μ-1,2-peroxo)Cu]$^{2+}$/MFI exhibit the same trend with 2[Cu(μ-O)Cu]$^{2+}$/MFI, the Cu$\cdots$O$_{peroxo}$ bond length is shortened from the range of 1.98-2.04 to 1.96-2.03 Å, and the average O$_{peroxo}\cdots$O$_{peroxo}$ bond length is shortened from 1.32 to 1.31 Å compared with the single active site model of [Cu(μ-1,2-peroxo)Cu]$^{2+}$/MFI (Table S4).
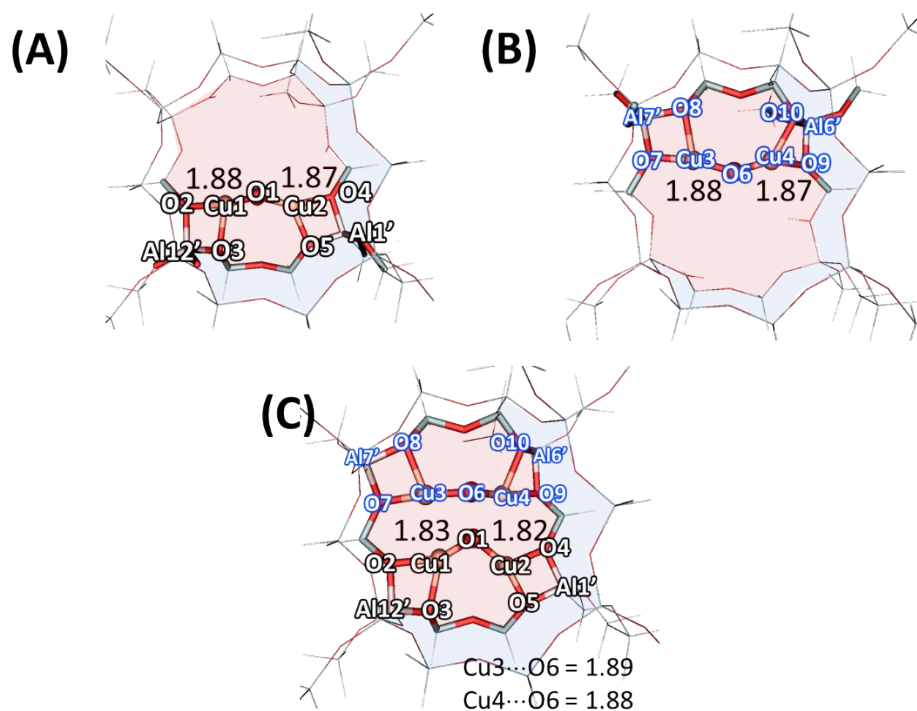
Fig. S3 Optimized structures for the single active sites of A) [Cu(μ-O)Cu]$^{2+}$@Al1'-Al12'/MFI, B) [Cu(μ-O)Cu]$^{2+}$@ Al6'-Al7' /MFI, and the double active sites of C) 2[Cu(μ-O)Cu]$^{2+}$/MFI calculated in the triplet spin ground state (Red and blue areas represent straight and zigzag channels, respectively, and the illustrated distance are in angstrom unit).
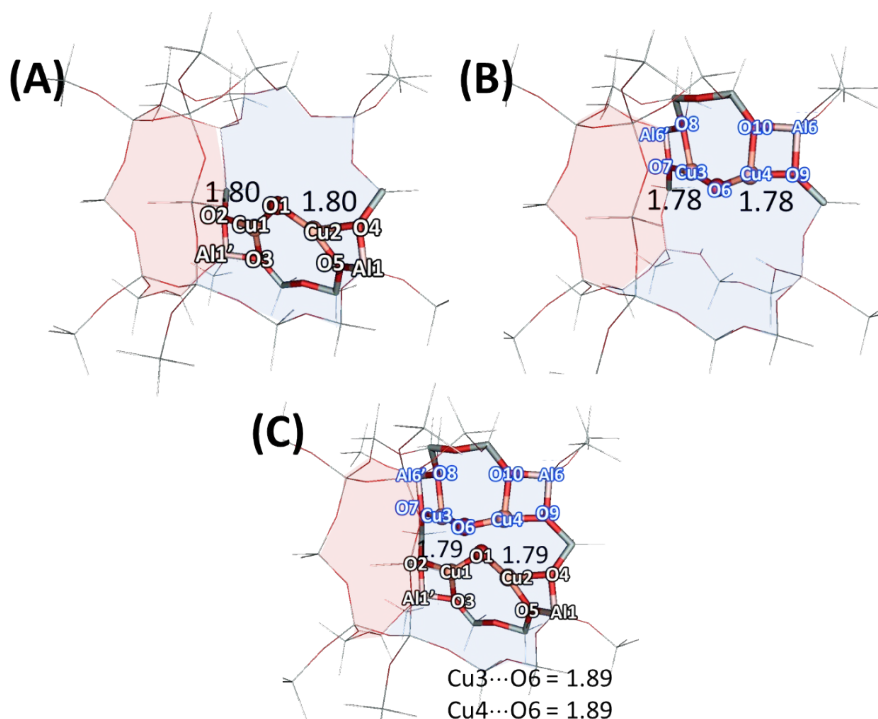
Fig. S4 Optimized structures for the single active sites of A) [Cu(μ-O)Cu]$^{2+}$@ Al1-Al1'/MFI, B) [Cu(μ-O)Cu]$^{2+}$@ Al6-Al6'/MFI, and the double active sites of C) 2[Cu(μ-O)Cu]$^{2+}$/MFI calculated in the triplet spin ground state (Red and blue areas represent straight and zigzag channels, respectively, and the illustrated distance are in angstrom unit).
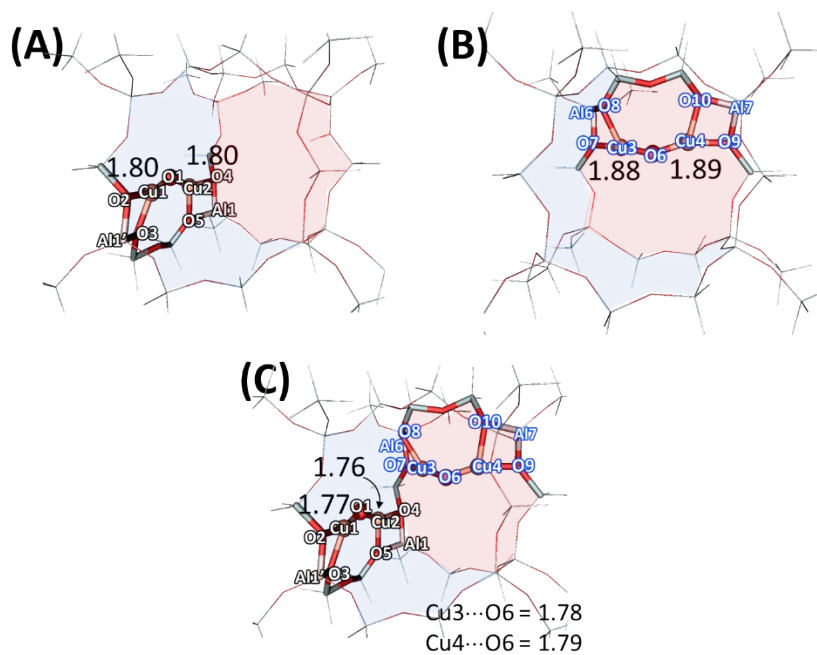
Fig. S5 Optimized structures for the single active sites of A) [Cu(μ-O)Cu]$^{2+}$@ Al1-Al1'/MFI, B) [Cu(μ-O)Cu]$^{2+}$@ Al6-Al7/MFI, and the double active sites of C) 2[Cu(μ-O)Cu]$^{2+}$/MFI calculated in the triplet spin ground state (Red and blue areas represent straight and zigzag channels, respectively, and the illustrated distance are in angstrom unit).
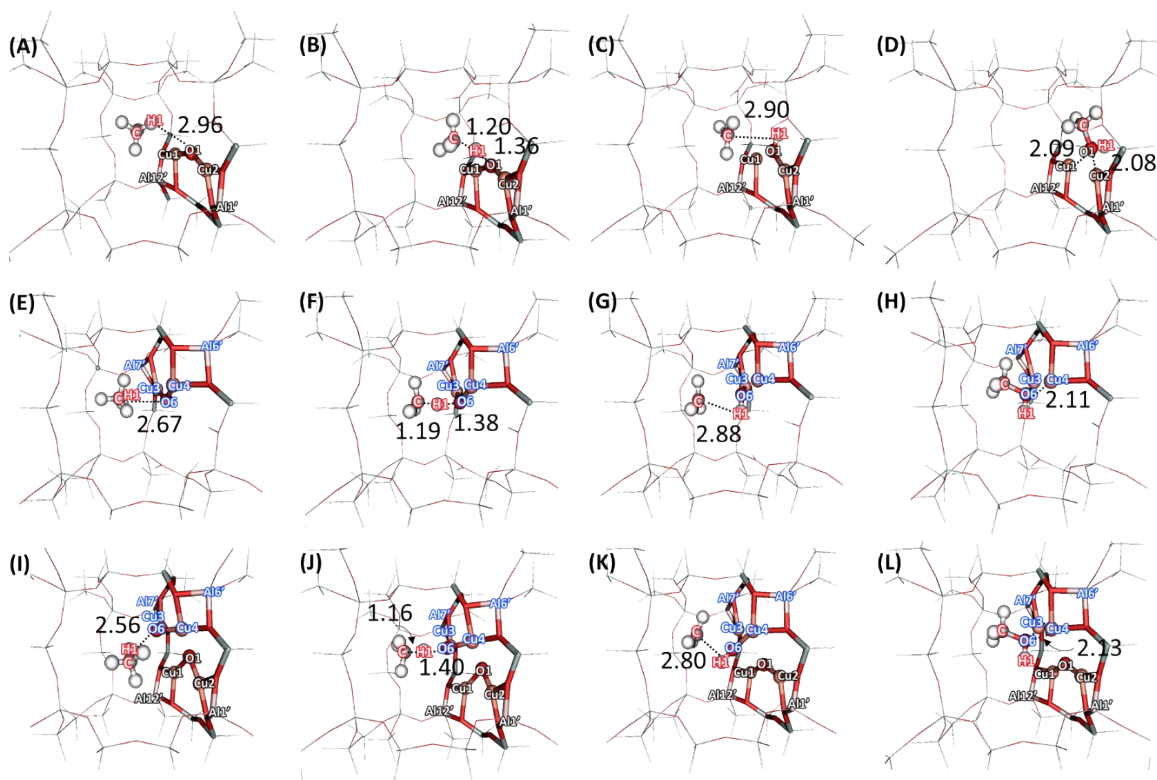
Fig. S6 Optimized structures of the overall steps of the direct conversion of methane to methanol on the single active sites of A-D) [Cu(μ-O)Cu]²⁺@Al1'-Al12'/MFI, E-H) [Cu(μ-O)Cu]²⁺@ Al6'-Al7' /MFI, and the double active sites of I-L) the double active sites of C) 2[Cu(μ-O)Cu]²⁺/MFI
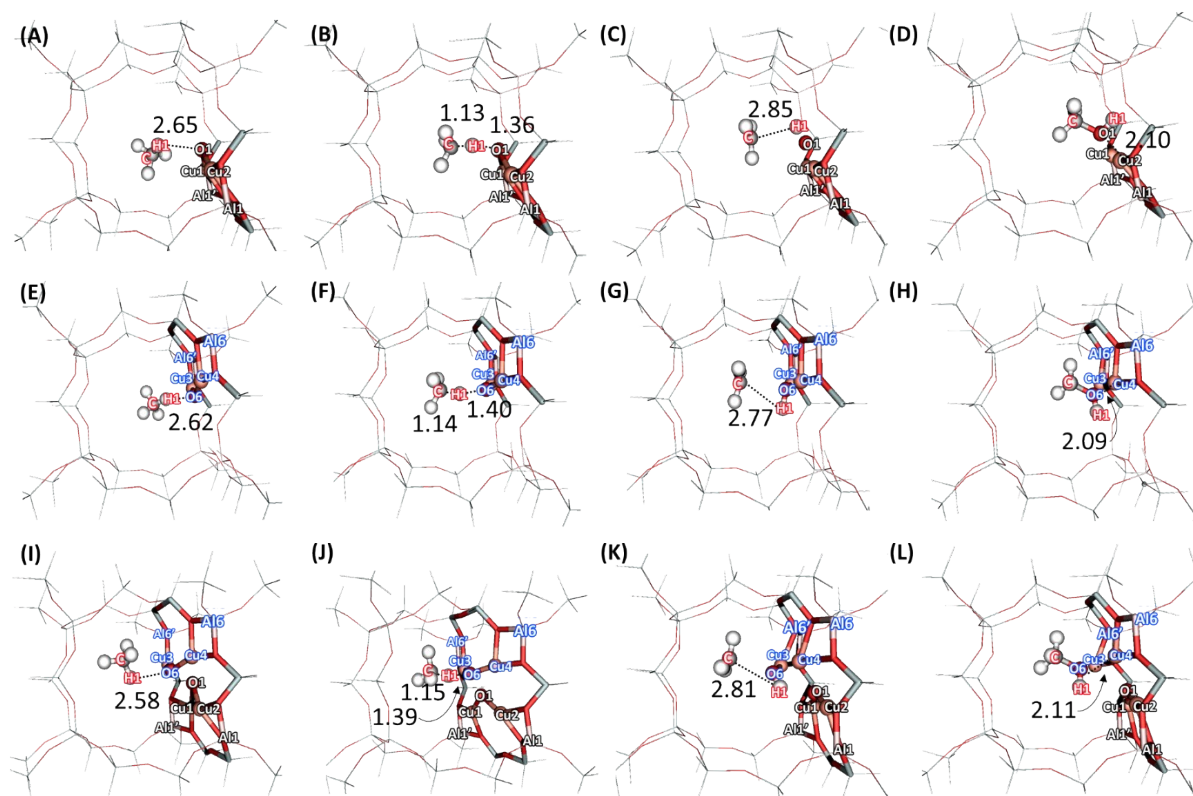
Fig. S7 Optimized structures of the overall steps of the direct conversion of methane to methanol on the single active sites of A-D) [Cu(μ-O)Cu]$^{2+}$@ Al1-Al1'/MFI, B), E-H) [Cu(μ-O)Cu]$^{2+}$@ Al6-Al6'/MFI, and the double active sites of I-L) the double active sites of C) 2[Cu(μ-O)Cu]$^{2+}$/MFI
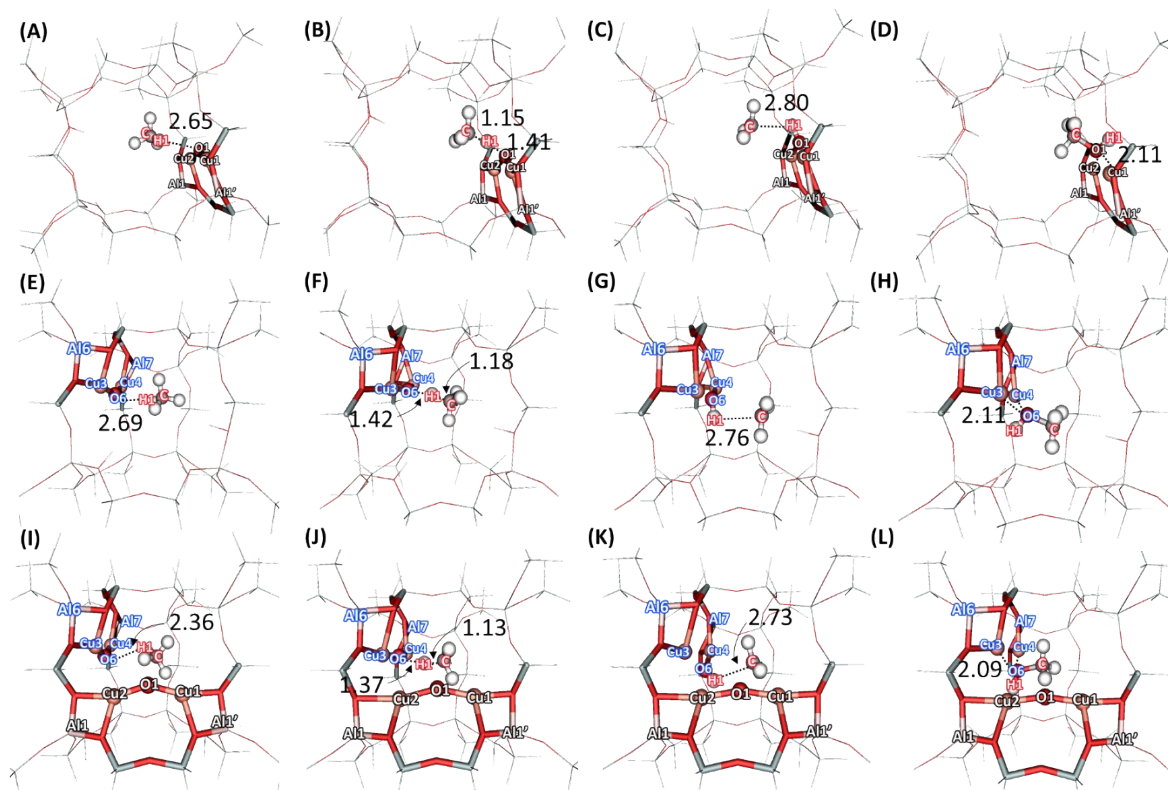
Fig. S8 Optimized structures Optimized structures of the overall steps of the direct conversion of methane to methanol on the single active sites of A-D) [Cu(μ-O)Cu]$^{2+}$@ Al1-Al1'/MFI, E-H) [Cu(μ-O)Cu]$^{2+}$@ Al6- Al7/MFI, and the double active sites of I-L) the double active sites of C) 2[Cu(μ-O)Cu]$^{2+}$/MFI

Fig. S9 Free energy profile ($\Delta G_{298.15}$) of overall steps of the direct conversion of methane to methanol on different Cu oxide clusters over MFI framework: A) comparison pathways of methane to methanol on single active site of [Cu(μ-O)Cu]2+@Al1'-Al12'/MFI (blue dash line), [Cu(μ-O)Cu]2+@Al6'-Al7'/MFI (red dot line), and on double active sites of 2[Cu(μ-O)Cu]2+/MFI (black line), B) comparison pathways on single active site of [Cu(μ-O)Cu]2+@Al1-Al1'/MFI (blue dash line), [Cu(μ-O)Cu]2+@Al6-Al6'/MFI (red dot line), and on double active sites of 2[Cu(μ-O)Cu]2+/MFI (black line), and C) comparison pathways on single active site of [Cu(μ-O)Cu]2+@Al1-Al1'/MFI (blue dash line), [Cu(μ-O)Cu]2+@Al6-Al7/MFI (red dot line), and on double active sites of 2[Cu(μ-O)Cu]2+/MFI (black line)

Table S1 Optimized geometrical parameters of the single active site of [Cu(μ-O)Cu]$^{2+}$@Al1'-Al12'/MFI

Parameters	ISO	ADS	TS1	INT	PROD
Distance (Å)					
Cu1-O1	1.89	1.79	1.86	1.97	2.23
Cu1-O2	1.86	1.98	1.88	2.24	2.03
Cu1-O3	1.95	2.02	1.97	2.07	2.12
Cu1-Al12'	2.69	2.74	2.69	2.79	2.73
Cu2-O1	1.88	1.77	1.86	1.80	1.99
Cu2-O4	1.85	1.95	1.86	1.93	1.96
Cu2-O5	1.97	2.03	2.00	2.00	1.88
Cu2-Al1'	2.72	2.77	2.72	2.74	2.70
C-Cu1	-	2.87	2.88	3.88	3.01
C-O1	-	3.68	2.59	3.11	1.50
C-H1	1.09	1.10	1.39	2.66	2.02
H1-O1	-	3.14	1.26	0.99	0.97
C-Cu2	-	4.68	3.86	3.90	2.98
Angle (°)					
Cu1-O1-Cu2	150.4	144.7	148.8	106.4	102.6

Table S2 Optimized geometrical parameters of the single active site of [Cu(μ-O)Cu]$^{2+}$@Al6-Al7/MFI

Parameters	ISO	ADS	TS1	INT	PROD
Distances (Å)					
Cu3-O6	1.90	1.78	1.93	1.78	2.11
Cu3-O7	1.87	1.95	2.22	1.96	2.08
Cu3-O8	1.98	2.08	2.02	1.97	2.09
Cu3-Al7	2.70	2.79	2.83	2.77	2.81
Cu4-O6	1.89	1.76	1.81	2.05	2.11
Cu4-O9	1.90	1.96	1.94	2.17	2.09
Cu4-O10	1.96	2.07	2.00	2.13	2.12
Cu4-Al6	2.65	2.65	2.66	2.73	2.73
C-Cu3	-	2.84	3.43	3.61	2.89
C-O6	-	3.06	2.58	2.70	1.46
C-H2	1.09	1.10	1.18	2.10	1.99
H2-O6	-	2.74	1.42	1.00	0.97
C-Cu4	-	4.42	3.83	3.05	3.06
Angle (°)					
Cu3-O6-Cu4	155.9	147.3	136.4	113.4	102.9

Table S3 Optimized geometrical parameters for the double active sites of 2[Cu(μ-O)Cu]²⁺/MFI

Parameters	ISO	ADS	TS1	INT	PROD
Distance (Å)					
Cu1-O1	1.77	1.78	1.85	1.99	2.09
Cu1-O2	2.00	1.98	2.00	2.07	2.14
Cu1-O3	2.01	2.02	2.06	2.16	2.08
Cu1-Al6	2.72	2.74	2.73	2.77	2.74
Cu2-O1	1.77	1.77	1.87	1.81	2.10
Cu2-O4	1.95	1.94	1.97	1.89	2.10
Cu2-O5	2.02	2.02	2.09	1.99	2.08
Cu-Al7	2.76	2.78	2.78	2.73	2.78
Cu3-O6	1.77	1.88	1.78	1.78	1.79
Cu3-O7	1.96	1.98	1.96	1.95	1.96
Cu3-O8	2.05	2.09	2.05	2.04	2.04
Cu3-Al7	2.77	2.78	2.78	2.77	2.77
Cu4-O6	1.78	1.86	1.78	1.77	1.79
Cu4-O9	1.96	1.96	1.96	1.95	1.96
Cu4-O10	2.05	2.11	2.05	2.05	2.05
Cu4-Al6	2.66	2.68	2.66	2.66	2.67
C-Cu1	-	2.85	3.16	3.21	2.95
C-O1	-	3.47	2.59	2.81	1.47
C-H1	1.09	1.10	1.18	1.88	2.00
H1-O1	-	2.73	1.43	0.99	0.97
C-Cu3	-	2.90	3.89	3.57	3.95
C-O6	-	3.02	3.13	2.87	3.06
C-H2	1.09	1.10	1.09	1.08	1.09
H2-O6	-	2.62	2.56	3.22	3.40
Angle (°)					
Cu1-O1-Cu2	141.5	143.7	131.5	129.5	95.3
Cu3-O6-Cu4	142.6	134.2	142.1	141.9	138.2

Table S4 Optimized geometrical parameters for the double active sites of 2[Cu(μ-1,2-peroxo)Cu]$^{2+}$/MFI

Parameters	ISO[a]	ISO	ADS	TS1	INT	PROD
Distance (Å)						
Cu1-O1	-	1.95	2.07	2.00	2.08	1.99
Cu1-O1'	-	2.87	2.87	2.81	2.94	2.84
O1-O1'	-	1.31	1.30	1.30	1.30	1.30
Cu1-O2	-	1.93	2.06	2.01	2.04	2.01
Cu1-O3	-	2.78	2.15	2.17	2.23	2.20
Cu1-Al12'	-	2.78	2.77	2.76	2.76	2.78
Cu2-O1	-	1.95	1.96	1.96	1.97	1.95
Cu2-O1'	-	1.97	1.98	1.99	1.98	1.97
Cu2-O4	-	1.91	1.97	1.92	1.93	1.91
Cu2-O5	-	1.96	1.93	1.98	2.00	1.96
Cu2-Al1'	-	2.66	2.75	2.74	2.76	2.74
Cu3-O6	2.04	2.03	2.04	2.03	2.02	1.92
Cu3-O6'	2.84	2.85	2.91	2.92	2.83	3.64
O6-O6'	1.32	1.30	1.31	1.40	1.45	2.64
Cu3-O7	2.02	2.02	2.02	2.05	2.04	2.06
Cu3-O8	2.18	2.19	2.22	2.23	2.22	2.19
Cu3-Al7	2.74	2.76	2.77	2.81	2.82	2.78
Cu4-O6	1.98	1.97	1.94	1.90	1.91	1.90
Cu4-O6'	1.99	2.00	1.98	2.07	2.02	1.97
Cu4-O9	1.96	1.95	1.93	1.96	1.93	2.02
Cu4-O10	1.97	1.97	1.97	1.97	1.99	1.99
Cu4-Al6	2.67	2.68	2.66	2.71	2.67	2.74
C-Cu1	-	-	2.66	3.46	2.31	5.20
C-O1	-	-	3.65	3.60	3.15	5.90
C-O1'	-	-	3.45	3.61	3.60	6.03
C-H1	-	-	1.10	1.09	1.09	1.09
H1-O1'	-	-	2.69	4.05	3.63	5.94
C-Cu3	-	-	2.95	4.47	4.47	3.83
C-O6	-	-	2.95	3.06	3.44	2.92
C-O6'	-	-	3.68	2.53	3.06	1.44
C-H2	1.09	1.09	1.10	1.35	3.53	2.01
H2-O6	-	-	2.67	2.06	1.95	3.57
H2-O6'	-	-	3.54	1.20	0.97	0.97
Angle (°)						

Cu1-O1'-Cu2	-	103.0	92.6	94.4	89.5	95.6
Cu1-O1-Cu2	-	157.1	124.3	128.9	120.9	133.5
Cu3-O6'-Cu4	96.8	96.7	95.6	89.2	89.9	66.7
Cu3-O6-Cu4	131.5	131.5	134.4	129.5	124.6	125.3

[a] Optimized geometrical parameters for the single active sites of [Cu(μ-1,2-peroxo)Cu]$^{2+}$/MFI

Table S5 Summarized Mulliken Charges of various Cu oxide cluster on Al1'-Al12' and Al6-Al7 pair in MFI framework through direct methane to methanol process.

Active sites	Fragment	ISO	ADS	TS	INT	PROD
[Cu(μ-O)Cu]$^{2+}$@Al1'-Al12'/MFI	Cu1	0.68	0.55	0.39	0.50	0.33
	Cu2	0.75	0.72	0.76	0.77	0.49
	O1	-0.83	-0.82	-0.69	-0.87	-0.60
	Spin	1	1	1	1	0
[Cu(μ-O)Cu]$^{2+}$@Al6-Al7/MFI	Cu3	0.69	0.67	0.72	0.71	0.68
	Cu4	0.65	0.57	0.25	0.45	0.33
	O6	-0.81	-0.81	-0.72	-0.87	-0.69
	Spin	1	1	1	1	0
2[Cu(μ-O)Cu]$^{2+}$/MFI	Cu1	0.71	0.55	0.46	0.47	0.45
	Cu2	0.61	0.72	0.49	0.49	0.41
	O1	-0.80	-0.82	-0.79	-0.82	-0.77
	Cu3	0.52	0.55	0.70	0.72	0.68
	Cu4	0.60	0.42	0.61	0.63	0.57
	O6	-0.56	-0.46	-0.81	-0.82	-0.77
	Spin	1	1	1	1	0
2[Cu(μ-1,2-peroxo)Cu]$^{2+}$/MFI	Cu3	0.26	0.21	0.24	0.29	0.25
	Cu4	0.69	0.73	0.73	0.75	0.70
	O6	-0.09	-0.12	-0.26	-0.33	-0.31
	O6'	-0.26	-0.29	-0.43	-0.48	-0.41
	Cu1	0.79	0.68	0.63	0.70	0.66
	Cu2	0.28	0.20	0.25	0.33	0.27
	O1	-0.13	-0.11	-0.10	-0.15	-0.13
	O1'	-0.30	-0.25	-0.27	-0.31	-0.28
	Spin	1	1	1	1	1

Table S6 Summarized Mulliken Charges of various Cu oxide cluster on Al1'-Al12' and Al6'-Al7' pair in MFI framework through direct methane to methanol process.

Active sites	Fragment	ISO	ADS	TS	INT	PROD
[Cu(μ-O)Cu]$^{2+}$@Al1'-Al12'/MFI	Cu1	0.70	0.55	0.39	0.51	0.34
	Cu2	0.76	0.73	0.75	0.78	0.50
	O1	-0.82	-0.81	-0.69	-0.86	-0.61
	Spin	1	1	1	1	0
[Cu(μ-O)Cu]$^{2+}$@Al6'-Al7'/MFI	Cu1	0.68	0.61	0.74	0.68	0.72
	Cu2	0.75	0.59	0.30	0.43	0.44
	O1	-0.82	-0.80	-0.69	-0.85	-0.65

Active sites	Fragment					
	Spin	1	1	1	1	0
2[Cu(μ-O)Cu]$^{2+}$/MFI	Cu1	0.65	0.56	0.46	0.52	0.48
	Cu2	0.58	0.68	0.49	0.49	0.45
	O1	-0.78	-0.80	-0.68	-0.81	-0.75
	Cu3	0.43	0.46	0.58	0.60	0.57
	Cu4	0.50	0.35	0.51	0.53	0.48
	O6	-0.47	-0.38	-0.73	-0.68	-0.64
	Spin	1	1	1	1	0

Table S7 Summarized Mulliken Charges of various Cu oxide cluster on Al1-Al1' and Al6-Al6' pair in MFI framework through direct methane to methanol process.

Active sites	Fragment	ISO	ADS	TS	INT	PROD
[Cu(μ-O)Cu]$^{2+}$@Al1-Al1'/MFI	Cu1	0.69	0.56	0.39	0.51	0.33
	Cu2	0.76	0.73	0.77	0.78	0.49
	O1	-0.84	-0.83	-0.70	-0.88	-0.61
	Spin	1	1	1	1	0
[Cu(μ-O)Cu]$^{2+}$@Al6-Al6'/MFI	Cu1	0.69	0.62	0.75	0.69	0.73
	Cu2	0.76	0.60	0.30	0.43	0.44
	O1	-0.83	-0.81	-0.68	-0.86	-0.66
	Spin	1	1	1	1	0
2[Cu(μ-O)Cu]$^{2+}$/MFI	Cu1	0.72	0.56	0.46	0.47	0.45
	Cu2	0.62	0.73	0.49	0.49	0.41
	O1	-0.81	-0.83	-0.80	-0.83	-0.78
	Cu3	0.53	0.56	0.71	0.73	0.69
	Cu4	0.61	0.42	0.62	0.64	0.58
	O6	-0.57	-0.46	-0.72	-0.83	-0.78
	Spin	1	1	1	1	0

Table S8 Summarized Mulliken Charges of various Cu oxide cluster on Al1-Al1' and Al6-Al7 pair in MFI framework through direct methane to methanol process.

Active sites	Fragment	ISO	ADS	TS	INT	PROD
[Cu(μ-O)Cu]$^{2+}$@Al1-Al1'/MFI	Cu1	0.70	0.57	0.40	0.52	0.34
	Cu2	0.78	0.74	0.79	0.80	0.50
	O1	-0.86	-0.85	-0.71	-0.90	-0.62
	Spin	1	1	1	1	0
[Cu(μ-O)Cu]$^{2+}$@Al6-Al7/MFI	Cu1	0.70	0.63	0.77	0.70	0.74
	Cu2	0.78	0.61	0.31	0.44	0.45
	O1	-0.85	-0.83	-0.69	-0.88	-0.67
	Spin	1	1	1	1	0
2[Cu(μ-O)Cu]$^{2+}$/MFI	Cu1	0.73	0.57	0.47	0.48	0.46
	Cu2	0.63	0.74	0.50	0.50	0.42
	O1	-0.83	-0.85	-0.82	-0.85	-0.80
	Cu3	0.54	0.57	0.72	0.74	0.70
	Cu4	0.62	0.43	0.63	0.65	0.59
	O6	-0.58	-0.47	-0.80	-0.85	-0.80
	Spin	1	1	1	1	0

Table S9 The activation energy and desorption energy reported by DFT calculation of the direct conversion of methane to methanol on various Cu oxide species and number of active site on MFI frameworks

Active site	Cu active site	Al site(s)	Computational method[a]	C-H cleavage mechanism	C-H activation barrier (kcal mol^{-1})	MeOH desorption energy (kcal mol^{-1})	Ref.
[CuO$^+$]	Single	10-MR(T1)	P/PBE-D2	Heterolytic	7.2	42.2	28
[Cu^2(μ-O)]$^{2+}$	Single	10-MR	C/B3LYP	Homolytic	18.5	-	11
	Single	8-MR(T7/T12)	P/PEB	Homolytic	22.2	37.3	26
	Single	10-MR	C/PBE	Homolytic	10.4	34.6	39
	Single	10-MR(T1/T1)	P/PBE-D2	Homolytic	17.0	50.8	27
	Single	10-MR(T3/T3)	P/PBE-D2	Homolytic	14.8	52.6	40
[Cu$_2$(μ-O)$_2$]$^{2+}$	Single	10-MR(T3/T3)	P/PBE-D2	Homolytic	12.0	19.8	40
[Cu$_3$(μ-O)$_3$]$^{2+}$	Single	8-MR(T7/T12)	P/PBE	Homolytic	12.9	20.6	26
[Cu(μ-O)Cu]$^{2+}$	Single	10-MR(T1'/T12')	C/M06-2X	Homolytic	22.9	75.9	this work
[Cu(μ-O)Cu]$^{2+}$	Single	10-MR(T6/T7)	C/M06-2X	Homolytic	19.5	74.6	this work
2[Cu(μ -O)Cu]$^{2+}$	double	10-MR (T1'/T12',T6/T7)	C/M06-2X	Homolytic	12.5	85.6	this work
2[Cu(μ-1,2-peroxo)Cu]$^{2+}$	double	10-MR (T1'/T12',T6/T7)	C/M06-2X	Homolytic	30.3	23.0	this work
[Cu$_2$O]$^{2+}$ Experiment	Single	-	C/B3LYP	Homolytic	15.7	-	11

[a] C and P stand for cluster model and periodic structure, respectively.